

# Fine structure above a light bridge in the transition region and corona

L. Bharti<sup>1\*</sup>

<sup>1</sup>*Bal Shiksha Sadan Society, Sajjan Nagar, Udaipur, Rajasthan, India*

Accepted ..... Received .....; in original form .....

## ABSTRACT

We present the results of multi wavelength, co-spatial and near co-temporal observations of jets above a sunspot light bridge. The data were obtained with the Solar Optical Telescope (SOT) on board Hinode, the Interface Region Spectrograph (IRIS) and the Atmospheric Imaging Assembly (AIA) on board the Solar Dynamic Observatory (SDO). Most of the jets in the Ca II H images show decreasing brightness with height while in the IRIS slit jaw images at 1330 Å jets show a bright leading edge. These jets show rising and falling motion as evident from the parabolic profile obtained from the time-distance diagram. The rising and falling speeds of the jets are similar. These jets show a coordinated behaviour between neighbouring jets moving jointly up and down. Some of the jets show a plasma ejection from the leading edge which is also hotter at the transition region (TR) and coronal temperatures. A similar behaviour is seen in the AIA wave bands that suggests that jets above the LB reach up to the lower corona and the leading edges are heated up to coronal temperatures. Such jets are important means of transfer mass and energy to the transition region and corona above sunspots.

**Key words:** Sun – convection, photosphere, chromosphere.

## 1 INTRODUCTION

Jet-like transients are assumed to be means of energy and mass transport from the solar surface to the upper layers of the solar atmosphere (Shibata et al. 2007, Morton et al. 2012).

\* E-mail: lokesh\_bharti@yahoo.co.in

High resolution observations from the Hinode/SOT have revealed numerous chromospheric anemone jets in the solar chromosphere outside active regions (Shibata et al. 2007). These jets have typical  $\lambda$ -shapes which supports the notion of reconnection between an emerging magnetic bipole and a preexisting uniform vertical field (Yokoyama & Shibata 1995) and gives indirect evidence of small-scale ubiquitous low-altitude reconnection in the solar atmosphere. There are also transient events of cool plasma such as spicules, macrospicules and surges (Beckers 1972, Koutchmy & Stellmacher 1976, Yamauchi et al. 2005) observed in the chromosphere. Spicules are observed **at** the limb in the chromospheric emission lines as well as in the UV and EUV wavelengths. From Hinode observations of de Pontieu et al. (2007a) the existence of two types of spicules, type-I and type-II, is identified. Both types of spicules are anchored to the photosphere. However, the driving mechanisms are different for both. Type-I spicules follow parabolic path as seen in the time-distance diagrams, suggesting that ejected mass returns to the solar surface while type-II spicules show accelerations and do not return to the surface at chromospheric temperatures. Pereira et al. (2014) show that they do return to the surface, but at transition region temperatures. Rouppe vander Voort et al. (2009) reported on the existence of type-II spicules on the solar disk.

Dynamic jet-like events are also observed above sunspots. Using limb observations from Hinode in the Ca II H band and TRACE at 1550 Å and 1600 Å Morton (2012) reported on jets at the edge of a sunspot which rises the chromospheric plasma to the low corona through the transition region (TR). The leading edges of jets show enhanced emission due to shock heating. Jet-like events above sunspot penumbrae 'penumbral micro jets' were reported by Katsukawa et al. (2007). Penumbral microjets are bright transients observed at the sides of penumbral filaments. Their apparent speed in the image plane is about 100 km/s and their lifetime are around one minute. It has been suggested that these jets are aligned with the more inclined penumbral field (Jurčák & Katsukawa 2008) and caused by reconnection between the more inclined penumbral field and background field. There are evidences of jet-like events in the sunspot umbra as well. Bharti et al. (2013) reported on the existence of umbral microjets. These jets are also aligned with the background magnetic field. These sub-arcsecond structures last for about one minute. Small-scale, jet-like features with periodic appearance in the chromosphere above sunspots has been found by Rouppe van der Voort & de la Cruz Rodríguez (2013). They originate due to the leakage of long-period waves into the chromosphere along inclined magnetic field. Yurchyshyn et al. (2013) described cool cone-shaped jet-like structures in the chromosphere above the strongest magnetic part of the

umbra. They show upward and downward oscillatory motion. According to these authors the driving mechanism of the jets are photospheric oscillations that generate upward moving shocks.

Brightness enhancement, ejection and surge activity above light bridges in the sunspot chromosphere have been also reported (Roy 1973, Asai et al. 2001, Bharti et al. 2007, Louis et al. 2008, 2009, Shimizu et al. 2009, Shimizu 2011). Shimizu et al. (2009) and Shimizu (2011) reported on a bright plasma ejection that was intermittent and recurrent for more than a day above a light bridge. Berger & Berdyugina (2003) reported on brightness enhancements above a light bridge in the transition region. Louis et al. (2014) suggested that jets above light bridges are guided by sunspot magnetic fields. These jets are caused by magnetic reconnection between the more inclined magnetic field in the LB and the more vertical umbral magnetic field. The presence of opposite polarity field close to these transient events is being hinted at by Bharti et al. (2007) and Louis et al. (2014).

## 2 OBSERVATIONS

The largest spot (NOAA active region 2192) of the current solar cycle was observed by IRIS, AIA/SDO and SOT/Hinode onboard on October 25, 2014. In the present study observations from these instruments from 05:17 UT to 06:30 UT are used. Slit-jaw images obtained by IRIS (De Pontieu et al. 2014) at 1330 Å (C II) with AN image scale of 0.166"/pixel and 7.3 sec cadence were obtained. The SDO/AIA (Lemen et al. 2012) observations have a plate scale of 0.6"/pixel and were taken with a cadence of 12 sec. G-band and Ca II H images obtained by Hinode (Kosugi et al. 2007) have an Image scale of 0.22"/pixel. Only a few G-band images are available. However, Ca II H images were taken every minute. The standard routine '*fg-prep.pro*' from solarsoft was applied to the Hinode data for flat field and dark current corrections. We used a Wiener filter to correct for the point spread function of the Hinode/SOT telescope. Calibrated Level 2 data from IRIS that include flatfield, darkcurrent and geometric corrections are used. Similarly, level 1.5 data from SDO/AIA are used. Hinode and AIA images were upscaled to the pixel scale of IRIS. The location of the spot on solar disk was at  $x = 319''$  and  $y = -328''$  which corresponds to a heliocentric angle  $\theta = 29^\circ$  ( $\mu=0.88$ ). The Ca II H and C II filter samples emission at  $10^4$  and  $\sim 3 \times 10^4$  K respectively. The AIA EUV channels cover the temperature range from  $6 \times 10^5$  K to  $2 \times 10^7$  K (Lemen et al. 2012).

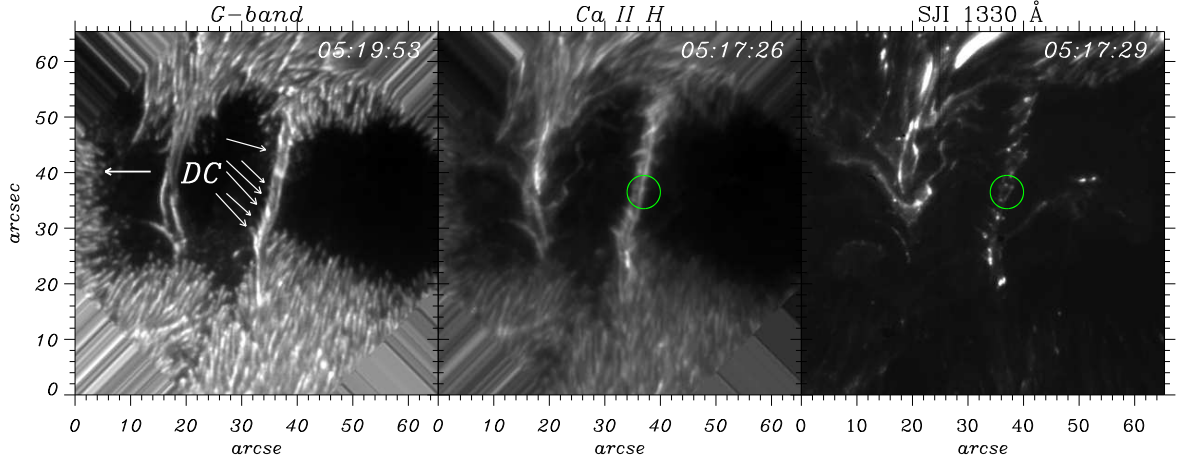


**Figure 1.** Left panel: G-band image of the observed sunspot at 05:19:53 UT. The disk center is indicated by the arrow labelled 'DC'. The arrows on the left side of the right LB indicates threads in the LB. Middle panel: co-spatial and near co-temporal Ca II H image at 05:17:26 UT. Right panel: IRIS slit-jaw image AT 1330 Å at 05:17:29 UT. The contrast has been enhanced in all images to show threads in G-band and brightening above them in Ca II H and IRIS slit-jaw images. Green circle indicates jets discussed in the main text.

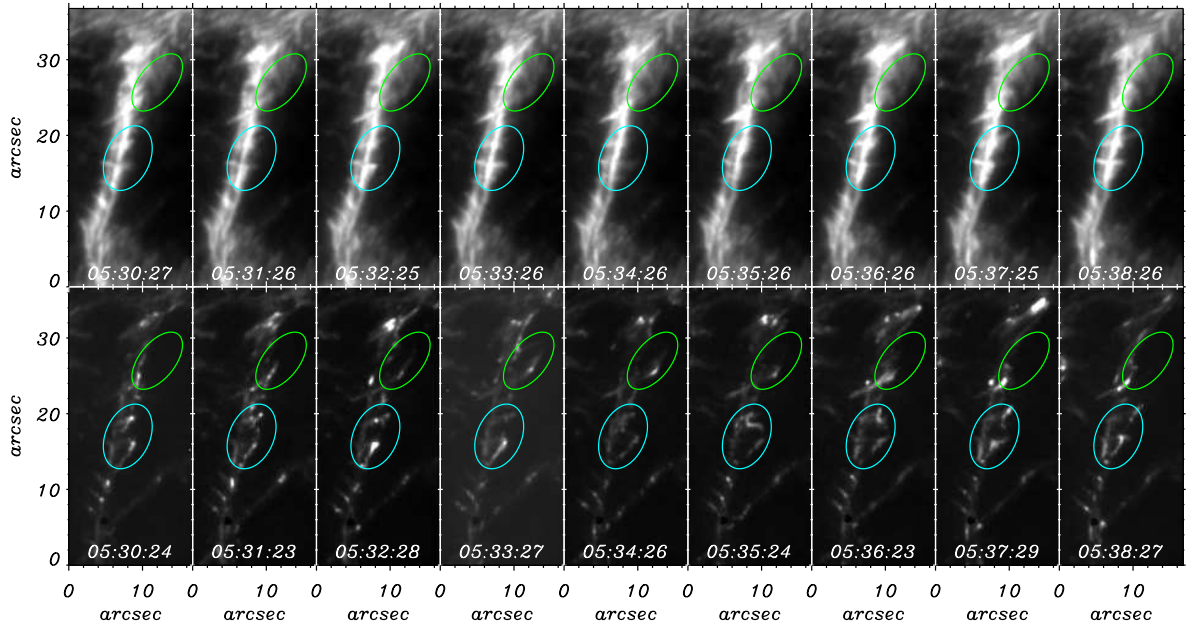


**Figure 2.** Evolution and interaction of jets above the LB. Upper row: Ca II H images; lower row: co-spatial and near simultaneous slit-jaw images at 1330 Å. The jet in the green ellipse rise and fall clearly. Merging and splitting of jets can be recognised in the cyan ellipse (see movie-II for more details which is available as on-line material).

### 3 ANALYSIS AND RESULTS

The left panel of Figure 1 shows a G-band image of the sunspot. This spot has two filamentary light bridges (LBs). The left one is broader than the right one. The central dark lane is more prominent in the broader one. We analyse the right LB in this study. There are

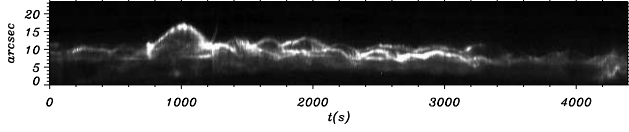


**Figure 3.** Time-distance diagram of a stationary slit for the whole span of observations in 1330 Å. The slit was oriented along the jet length. The location of this jet is indicated by the green ellipse in Figure 2 that achieves maximum height around 1000 sec. The parabolic profiles of jets indicates that ejected jet mass returns.

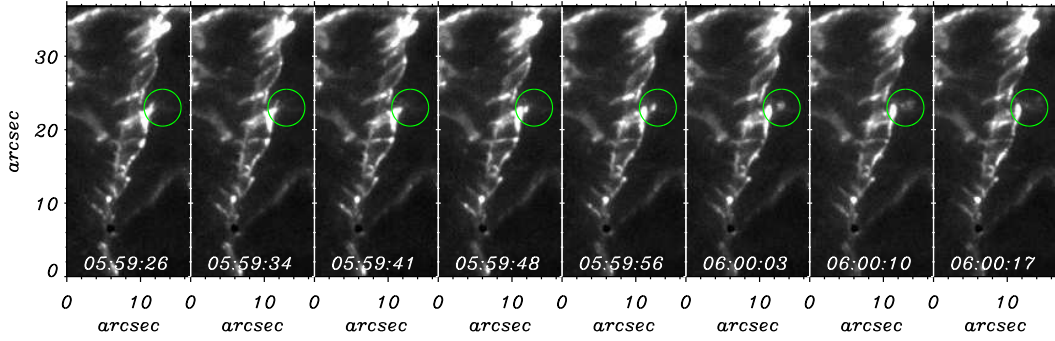


**Figure 4.** Evolution and migration of a bright blob as a result of interaction of jets, seen in the IRIS slit-jaw images (see Movie II for more details which is available as online material). The contrast of the images has been enhanced to see the fading of the bright ejection in the umbral background.

several thread-like structures on the left side of this LB. The locations of these structures are indicated by arrows. These structures also have central dark lanes, similar to penumbral filaments and LBs. The end points lie in the dark umbra. A co-spatial Ca II H image from about two and half minutes earlier than the G-band image is displayed in the middle panel. The right LB shows bright jet-like structures at both the left and right sides. These brightening can be seen in movie-I, available in the online version. The thread-like structures in the G-band image also appear brighter in the Ca II H images and there is always enhanced

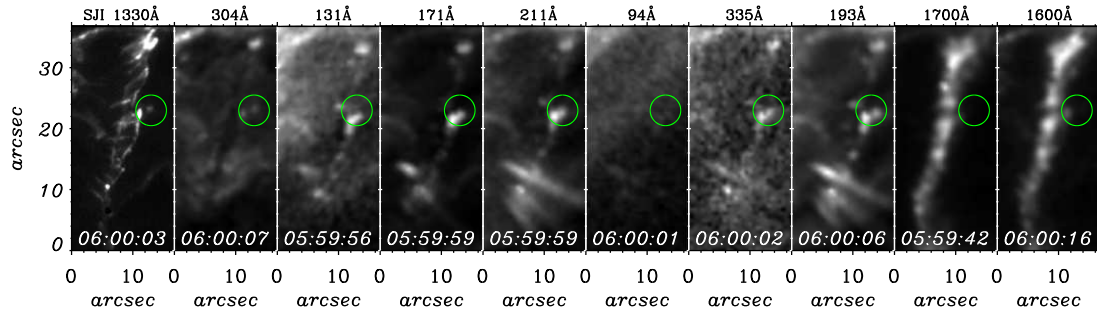


**Figure 5.** Co-spatial and near co-temporal images of the LB in various wave bands. The leftmost image shows the IRIS slit-jaw image at 1330 Å, after that AIA images in various wave bands are displayed. The green circle indicates the location of the bright ejection shown in Figure 4. The ejected mass as well as the leading edge of jets are also bright at coronal temperatures.

brightening on the left side of the LB. Since disk center is towards the left side of the LB, jet-like structures in the Ca II H images on the right side of the LB are more distinct in the dark umbral background. The right panel illustrates a co-spatial and near simultaneous IRIS slit-jaw image (SJI) at  $1330 \text{ \AA}$ . Thread-like structures are also bright in SJI but some of them have bright plasma blobs. These thread-like structures have been chosen as a reference to co-align the Hinode and SIJ images. Close inspection of movie-II which is available as online material suggests that these blobs indicate apparent loop-like shapes which rise and fall back down. Limited spatial resolution hinders identifying further details. The most notable features of SJI is that the jets have bright leading edges on the right side of the LB. Some jets show only a bright base and the bright leading edge and a void in between. On the other hand some jets show hazy regions in between. Examining these jets in the Ca II H image shows only a few hazy structures. A right triangular-like structure can be seen at  $x = 38''$  and  $y = 38''$  in the SJI image (indicated by a green circle) where opposite is one distinct jet and hypotenuse show the bright leading edges. In the Ca II H image only hazy opposite is hinted. The leading edges of the jets form a chain like structure in the SJI images. To our knowledge such a behaviour of jets above a LB in TR lines have not been reported earlier. We cannot rule out the possibility that there are distinct jets (Louis et al. 2014) and due to the lower resolution of the Ca II H data they are not visible. Moreover, due to the limited spatial resolution of IRIS, the bright leading edge of each jet is not clearly visible even in the SJI. Only a chain of leading edge is visible in the SJI.

Figure 2 demonstrate the evolution of jets in both the  $1330 \text{ \AA}$  and Ca II H lines. All images are spatially co-aligned and near co-temporal. We first discuss the rise and fall of a jet whose location is shown by green ellipse in both wave bands. At 5:30 UT two chain-like structures can be seen in the  $1330 \text{ \AA}$  image at the left side of the ellipse. The lower chain is brighter than the upper one while the lower part of the lower chain is connected to the base of the LB. The less brighter chain is isolated i.e. only leading edges can be seen. In the Ca II H image these structure appear differently. Both structures are distinct and jet-like. The bright chain is still brighter in the Ca II H. Both have bright bases but the brightness decreases with height for the upper jet. With time the length of both jets increases and they appear like a loop in the  $1330 \text{ \AA}$  band while in the Ca II H band, instead of two distinct jets, they form a hazy blob. At 5:34 UT the jet approaches to the maximum height and then starts to fall. Notice that there is still a hazy blob in the Ca II H. The apparent maximum length of the apparent loops is about 2100 km. Interaction of jets in the terms of merging

is indicated by a cyan ellipse. Initially, at 5:30 UT two distinct chains of leading edges are seen in the 1330 Å image. The lower chain is broader and longer. These chains appear very different in Ca II H. There are two distinct jets can be seen from which the upper one is brighter. With time the jets rise and merge with each other. At 5:36 UT they show a one chain system in 1330 Å. After that they again show two chain systems from which the upper one rises again. The notable difference is that these jets appears only as hazy blob structures and at some instance as jet-like in the Ca II H.

Figure 3 demonstrates a space-time diagram of a jet. This jet is labeled by the green ellipse in Figure 2. A stationary slit is put along the jet length. The slit is put for the total time span so that rising and falling speeds as well as trajectories of other jets can be identified. The jet approaches to the maximum height around  $T=1000$  sec. The projected rising speed of this jet is  $\approx 12$  km/s and the falling speed is  $\approx 13$  km/s. Thus the rising and falling speeds are similar. A similar behaviour can be seen for other jets too. Apart from the striking rising and falling motion, jets reoccur around the same location over the full observational period and a coordinated behavior of neighboring jets moving up and down can be detected. Such behaviour of jets (dynamic fibrils) have been reported in sunspots (Rouppe van der Voort & de la Cruz Rodríguez 2013) and plage (Hansteen et al. 2006, De Pontieu et al. 2007) in the chromospheric lines.

Figure 4 illustrates the mass ejection from a jet. In movie-II one can see that before 5:59:26 UT there were two different leading edges of jets. The lower jet migrates towards the upper one and starts to merge with it. At 5:59:34 UT the merging completes and later on a plasma blob detaches from it. The blob moves away from leading edge and after 6:00:17 UT it fades away. Thus the lower rising jet pushes a pre-existing jet, destabilizes it and an ejection occurs. This event can be seen only in the 1330 Å images. Such finer details at high spatial and temporal scale is only possible due to IRIS capability.

### 3.1 Relation to photospheric flow

The Ca II H as well as 1330 Å movies suggest that bright jets migrate from the center of the LB towards both sides to the nearby penumbra. A G-band movie with an uneven cadence and only a few images as well as a HMI continuum movie (not shown here) also show such migration of mass from the center of the LB towards the nearby penumbra. Such a flow pattern and its relation with chromospheric brightening is also found by Bharti et al.

(2015a) and Louis et al. (2008, 2014). Also the orientation of the jets towards the penumbra suggests that these jets follow magnetic field lines which are more inclined in the in the penumbra (Louis et al. 2014).

### 3.2 Correlation with AIA wavelengths

The same LB is also observed in the AIA wavebands. Since the observed jets above LB in the 1330 Å are different or not resolved in the Hinode Ca II H images, it is imperative to see their appearance in AIA channels. The leading edges seen in the SJI also appear brighter than the umbral background in the AIA images. They are used as a reference for co-alignment in an approximate manner. The plasma ejection event displayed in Figure 4 at 6:00:03 UT is shown in Figure 5 in various wavebands. In the 304 Å image all jet-like structures appear darker from the bottom to top, only the leading edges appear bright in the 304 Å. The plasma ejection event (bright leading edge and detached plasma blob) indicated by a green circle is also brighter. Similarly, the leading edge of the jet at  $x = 12''$  and  $y = 34''$  is also bright while the lower part of the jet is still dark. A movie of the 304 Å images (movie-III IS available as online material) show dark material falling down above LB at  $x = 13''$  and  $y = 12''$  from 5:23:07 UT to 5:32:56 UT. In the 131 Å image only the leading edges of the jets appear brighter. Since the 131 Å image has been obtained approximately 7 sec earlier, the location of ejection event is shifted. Note that there is a shift also due to the projection effect of formation height of different wavebands. The structuring in the 171 Å and 211 Å images are similar as only the leading edges are visible. Some bright loops from the umbral core are also visible above the LB structure. There are no signatures of jets in the 94 Å image. In the 335 Å image only the leading edges are discernible. However, a loop from the umbra at  $x = 6''$  and  $y = 13''$  is hinted. The visibility of the leading edges and umbral loops above the LB is similar to that in the 171 Å, 211 Å and in the 193 Å image. The bright part of the coronal loops seen in the umbra are plumes (Foukal 1978). A detailed analysis of plumes has been presented by Kleint et al. (2014) using IRIS spectra. The structuring of the LB in the 1700 Å image is similar to that in Ca II H but due to the lower resolution of AIA fine structures are not clear. Even bright threads seen in the G-band and Ca II H are not visible. The bright threads as well as the bright leading edges are also visible in the 1600 Å image. Berger & Berdyugina (2003) reported enhanced contrast above a LB structure



in the 1600 Å images taken from the TRACE. The resolution of their data was not high enough to resolve the fine scale details observed by IRIS.

## 4 DISCUSSION AND CONCLUSION

With high spatial and temporal resolution slit jaw images from the IRIS at 1330 Å we are able to demonstrate fine scale details of jets above a LB in the TR which were hidden in earlier observations from the ground and from space. Particularly even at the double resolution of Ca II H images from Hinode such fine details and structuring have not been seen. Louis et al (2004) presented a detailed study of chromospheric jets above a LB that show triangular shaped blobs. The top part of the jets extend into a spike-like structure. Thus such spikes have a bright base and the top part is extended into the dark umbral background with decreasing brightness toward outer edge. This is the general brightness structure of the Ca II H jets. However, some jets show the bright leading edge as well. The main difference found in the present analysis belongs to the 1330 Å images. In most of the cases only the bright leading edge of the jets are seen in the dark umbral background with high contrast. The section of jets between the apex and the base is almost void in the 1330 Å while no such void is seen in the Ca II H images. Only very bright jets show continuous structure in the 1330 Å similar to the Ca II H.

Jets, blobs or brightening seem to be essential parts of the chromosphere above LBs. However, Bharti et al. (2015 in preparation) suggested that such activity is preferentially seen above filamentary LBs. Lagg et al. (2014) analysed a granular LB and did not find such activity in the Ca II H images. Low altitude reconnection has been suggested as mechanism to produce such an activity (See Bharti et al. 2007 and reference their in). According to recent MHD simulations, sunspot fine structures are caused by magnetoconvection. Cheung et al. (2010) has shown that simulated LBs have upflows in the central part and downflows at the lateral edges similar to penumbral filaments. These strong downflows at the lateral edges drags field lines and forms a hairpin like structure with opposite polarity (Bharti et al. 2010, Rempel et al. 2011). Such opposite polarity fields have been reported in penumbral filaments by Franz & Schlichenmaier (1013) and Scharmer et al. (2013). With new inversion schemes where the PSF of the telescope has been taken into account, more opposite polarity fields are reported (Ruiz Cobo & Asensio Remos 2013, van Noort 2012). Using synthetic spectra from a simulated sunspot Bharti et al. (2015) confirmed this scenario. Bharti et al.

(2015b) find a significant amount of opposite polarity field at the lateral edges of LBs using spatially coupled inversion (van Noort 2012) on Hinode/SP data that is accompanied with brightening in Ca II H. Louis et al. (2014) also reported isolated patches of opposite polarity around the location of jets observed in Ca II H. Bharti et al. (2015a) reported  $\lambda$ -shaped jets above a LB in the Ca II H images observed at the SST and opposite polarity patches in the photospheric magnetic field at the edge of the LB. Thus reconnection occurs between a newly emerged opposite polarity patch and the preexisting umbral field. Such a reconnection scenario is suggested to explain jets (or  $\lambda$ -shaped jets) seen in the chromosphere (Yokoyama & Shibata 1995, Shibata et al. 2007). Thus triangular shaped jets reported by Louis et al. (2014) could be  $\lambda$ -shaped and jets reported by Bharti et al. (2015a) could be more clear due to the higher resolution of the SST data and the advantageous viewing angle. We also clearly see the effect of the viewing angle on the data presented here as jets are seen only on the right side (opposite side of disk center) of the LB, laying over the umbral background. There are hints of  $\lambda$ -shaped jets but viewing angle and resolution is not ideal to see them distinctly. The spatial and temporal resolution of IRIS data is good enough to detect small scale dynamics such as mass motion and loop interaction which was not possible from Hinode Ca II H data (Louis et al. 2014). Using the Ca II H Hinode/SOT observations Shimitzu et al. (2009) and Shimitzu (2011) reported about intermittent plasma ejections above a LB for a few days, accompanied with a change in the photospheric magnetic flux density and inclination. Shimizu (2009) proposed a model where the LB is considered as a highly twisted current-carrying flux tube lying below the background field that forms a cusp-like shape above the LB. The proposed geometry then produces opposite polarity field at one side of LB and led to reconnection. Numerical simulations by Magara (2010) and Nishizuka et al. (2012) succeeded to produce jet-like structures in a penumbral configuration (Katsukawa et al. 2007) where reconnection occurs between the more horizontal penumbral and more vertical background field. This scenario is similar in the case of a LB having horizontal field and slightly inclined umbral field (Jurčák et al. 2006).

The main findings of the current study are enhanced emission along the leading edge of jets and coordinated behavior between neighbouring jets observed in the IRIS and AIA wavebands. Rouppe van der Voort & de la Cruz Rodríguez 2013) find jets (dynamic fibrils with parabolic path) whose properties vary from the sunspot umbra to beyond the penumbra. This reinforces the role of convective energy and inclination on the propagation of long period waves that form shocks in the chromosphere. However, these jets are found to be different

from penumbral micro-jets (Katsukawa et al. 2007) and umbral micro-jets (Bharti et al. 2013) which are caused by reconnection. The LB jets studied here are caused by reconnection and we speculate that a wave phenomenon (leakage of waves through the LB) is responsible for the coordinated behavior between neighbouring jets. Morton (2012) reported on jets at the edge of a sunspot in Ca II H Hinode observations and suggested that the enhanced emission is caused by shock heating. Thus plasma is heated by a shock front at TR temperatures around the leading edge of the jets and only the leading bright edge is visible in most of the LB jets. However, we cannot rule out other mechanisms and topologies that can just compress the jet material, i.e., increases its density, which, under optically thin conditions, leads to increased emission (Morton 2015, private communication). The remaining part of the jets remain cooler in the TR. Some jets in the Ca II H images show an entire bright structure with the leading edge which indicates that jets are at chromospheric temperature. The coronal counterpart of the jets also show the same behaviour, as evident from the 211 Å and 193 Å images that only the leading edges appear brighter. Thus the jet's leading edges are heated up to coronal temperatures. However, these channels also contain significant TR contribution, which may well be the cause for the observed brightness. In the TR the most part of the jet is as cool as the ambient umbra so the it is hardly visible while the leading edges are at TR temperatures, thus they appear bright. The lack of visibility of the body of the jets in the 1330 Å passband may be caused by the fact that the passband contains both FUV continuum that is formed at lower chromospheric temperatures (likely the reason of the bright bottom of the jets in C II) as well as the C II lines which are formed at the upper chromospheric/low TR temperatures, thus the leading edges appear brighter. The ejected blobs of plasma seen bright in the TR and coronal wavelength bands are also sources of mass and heat. This suggests that such jets are important media to transfer energy from the photosphere to the corona via the TR above the sunspot.

Spectral analysis of LB jets and their leading edge from the IRIS spectra in various wavelengths will be useful to understand various properties of these small scale dynamic jets (Bharti et al. in preparation).

## ACKNOWLEDGMENTS

The author thanks anonymous referee for useful criticism to improve the presentation of this manuscript. Dr. J. Hirzberger gratefully acknowledged for carefully reading the manuscript.

IRIS is a NASA small explorer mission developed and operated by LMSAL with mission operations executed at NASA Ames Research center and major contributions to downlink communications funded by the Norwegian Space Center (NSC, Norway) through an ESA PRODEX contract. Hinode is a Japanese mission developed and launched by ISAS/JAXA, collaborating with NAOJ as a domestic partner and NASA and STFC (UK) as international partners. Scientific operation of the Hinode mission is conducted by the Hinode science team organized at ISAS/JAXA. This team mainly consists of scientists from institutes in the partner countries. Support for the postlaunch operation is provided by JAXA and NAOJ (Japan), STFC (UK), NASA, ESA, and NSC (Norway).

## REFERENCES

- Asai, A., Ishii, T., Kurokawa, H. 2001, *ApJ*, 555, L65
- Beckers, J. M. 1972, *ARA&A*, 10, 73
- Berger, T. E., Berdyugina, S. V. 2001, *ApJ*, 589, L117
- Bharti, L., Solanki, S. K., Hirzberger, J. 2015a, submitted to *ApJ*
- Bharti, L. & Rempel, M., 2015b, submitted to *ApJ*
- Bharti, L., Hirzberger, J., Solanki, S. K. 2013, *A&A*, 552, L1
- Bharti, L., Beek, B., Schüssler, M. 2010, *A&A*, 510, 12
- Bharti, L., Rimmele, T., Jain, R., Jaaffrey, S. N. A., Smartt, R. N. 2007, *MNRAS*, 376, 1291
- Cheung, M. C. M., Rempel, M., Title, A. M., Schüssler, M. 2010, *ApJ*, 720, 233
- De Pontieu, B., Title, A. M., Lemen, J. R., et al. 2014, *Solar Phys.*, 289, 2733
- De Pontieu, B., McIntosh, S., Hansteen, V. H., et al. 2007, *PASJ*, 59, 655
- De Pontieu, B., Hansteen, V. H., Rouppe van der Voort, L., van Noort, M., & Carlsson, M. 2007a, *ApJ*, 655, 624
- Foukal, P.V. 1978, *ApJ*, 223, 1046
- Franz, M. & Schlichenmaier, R. 2013, *A&A*, 550, 97
- Hansteen, V. H., De Pontieu, B., Rouppe van der Voort, L., van Noort, M., & Carlsson, M. 2006, *ApJL*, 647, L73
- Jurčák, J., Katsukawa, Y. 2008, *A&A*, 488, L33
- Jurčák, J., Martínez Pillet, V., Sobotka, M., 2006, *A&A*, 453, 1079
- Katsukawa, Y. et al. 2007, *Science*, 318, 1594
- Kleint, L. et al. 2014, *ApJ*, 789, L42
- Koutchmy, S. & Stellmacher, G. 1976, *Sol. Phys.*, 49, 253
- Kosugi, T. et al. 2007, *Solar Phys.*, 243, 3
- Lagg, A., Solanki, S., K., van Noort, M., Danilovic, S. 2014, *A&A*, 568, A60
- Lemen, J. R., Title, A. M., Akin, D. J. et al. 2012, *Solar Phys.*, 275, 17
- Louis, R. E., Beck, C., Ichimoto, K. 2014, *A&A*, i567, 96
- Louis, R. E., Bellot Rubio, L. R., Mathew, S. K., Venkatakrishnan, P. 2009, *ApJ*, 704, L29
- Louis, R. E., Bayanna, A. R., Mathew, S. K., Venkatakrishnan, P. 2008, *Sol. Phys.*, 252, 43
- Magara, T. 2010, *ApJ*, 715, L40
- Morton, R. J. 2012, *A&A*, 543, 6
- Nishizuka, N., Hayashi, Y., Tanabe, H., Kuwahata, A., Kaminou, Y., Ono, Y., Inomoto, M., Shimizu, T. 2012, *ApJ*, 756, 152
- Pereira et al. 2014, *ApJ*, 792, L15

- Rempel, M. 2011, ApJ, 729, 5
- Rouppe van der Voort, L. & de la Cruz Rodríguez, J., 2013, ApJ, 776, 56
- Rouppe van der Voort, L., Leenaarts, J., de Pontieu, B., Carlsson, M., Vissers, G. 2009, ApJ, 705, 272
- Roy, J. 1973, Sol. Phy., 28,95
- Ruiz Cobo, B., Asensio Ramos, A. 2013, A&A, 549, L4
- Scharmer, G. B., de la Cruz Rodríguez, J., Sütterlin, P., Henriques, V. M. J. 2013, A&A, 553, 63
- Shibata, K., Nakamura, T. et al. 2007, Science, 318, 1591
- Shimizu, T. 2011, ApJ, 738, 83
- Shimizu et al. 2009, ApJ, 696, 66
- van Noort, M. 2012, A&A, 548, 5
- Yamauchi, Y., Wang, H., Jiang, Y., Schwadron, N., Moore, R. L. 2005, ApJ, 629, 572
- Yurchyshyn, V., Abramenko, V., Kosovichev, A., Goode, P. 2014, ApJ, 787, 58
- Yokoyama, T., Shibata, K., 1995, Nature, 375, 42